Inhibition of melanoma cell motility by the snake venom disintegrin eristostatin

Jing Tian[a], Carrie Paquette-Straub[a], E. Helene Sage[b], Sarah E. Funk[b], Vivek Patel[c], Deni Galileo[c], Mary Ann McLane[a],*

[a]*Department of Medical Technology, University of Delaware, 305G Willard Hall, Education Building, Newark, DE 19716, USA*
[b]*Hope Heart Program, Benaroya Research Institute at Virginia Mason, Seattle, WA 98101, USA*
[c]*Department of Biological Sciences, University of Delaware, 232 Wolf Hall, Newark, DE 19716, USA*

Abstract

Eristostatin, an RGD-containing disintegrin isolated from the venom of *Eristicophis macmahoni,* inhibits lung or liver colonization of melanoma cells in a mouse model. In this study, transwell migration and *in vitro* wound closure assays were used to determine the effect of eristostatin on the migration of melanoma cells. Eristostatin significantly impaired the migration of five human melanoma cell lines. Furthermore, it specifically inhibited cell migration on fibronectin in a concentration-dependent manner, but not that on collagen IV or laminin. In contrast, eristostatin was found to have no effect on cell proliferation or angiogenesis. These results indicate that the interaction between eristostatin and melanoma cells may involve fibronectin-binding integrins that mediate cell migration. Mutations to alanine of seven residues within the RGD loop of eristostatin and four residues outside the RGD loop of eristostatin resulted in significantly less potency in both platelet aggregation and wound closure assays. For six of the mutations, however, decreased activity was found only in the latter assay. We conclude that a different mechanism and/or integrin is involved in these two cell activities.
© 2007 Elsevier Ltd. All rights reserved.

Keywords: Disintegrin; Integrin; Melanoma; Migration; Fibronectin; Extracellular matrix; Alanine mutations

1. Introduction

Disintegrins are a family of low molecular weight and cysteine-rich proteins derived from viper venom. They were first identified as inhibitors of platelet aggregation and were subsequently shown to antagonize fibrinogen binding to platelet integrin $\alpha IIb\beta3$ (Gould et al., 1990; Ouyang et al., 1983).

Most disintegrins possess binding motifs (RGD, KGD, MVD, MLD, and VGD) similar to those found in fibronectin, fibrinogen and VCAM-1 (McLane et al., 2004). They bind to various integrins with high affinity, and always inhibit the binding of the natural ligand. Although disintegrins are highly homologous, significant differences exist in their affinity and selectivity for integrins.

Eristostatin, a RGD-containing 49-residue disintegrin isolated from the venom of *Eristicophis macmahoni,* potently inhibits human platelet aggregation initiated by ADP (McLane et al., 1994).

*Corresponding author. Tel.: +1 302 831 8737; fax: +1 302 831 4180.

E-mail address: mclane@udel.edu (M.A. McLane).

Previous studies indicate eristostatin (at 25 µg/mouse) inhibits liver and lung colonization when injected simultaneously with B16F10 murine melanoma cells into the tail vein of C57BL/6 mice (Beviglia et al., 1995; Morris et al., 1995). Danen et al. (1998) found that eristostatin inhibits lung colonization following intravenous injection of MV3 human melanoma cells in nude mice, whereas we have demonstrated that eristostatin (at 10 µg/mouse) inhibits lung colonization of two other human metastatic melanoma cells: M24met and C8161 (McLane et al., 2003). The mechanism by which eristostatin inhibits murine and human melanoma cell functions is unknown.

Before cancer cells form a new tumor, they must escape from the primary site, enter the bloodstream, and survive blood flow. They must arrest in a distant organ, then survive and proliferate in the foreign microenvironment (Couzin, 2003). Integrins are the major receptors for cell adhesion to extracellular matrix (ECM) proteins. Many of these metastatic steps involve integrin–ECM interaction, such as cell adhesion, migration, survival and proliferation at secondary sites (Giancotti, 1997; Jin and Varner., 2004). Disintegrins bind to integrins and interfere with integrin function (McLane et al., 2004). We propose that eristostatin prevents melanoma cell colonization of lung or liver via its blockage of integrin–ligand interaction.

In this study, we asked whether eristostatin modulates cell migration through integrins. Cell migration is known to involve integrins (Giancotti, 1997) and cell migration can contribute to tumor cell metastasis (Ridley et al., 2003). In previous studies we showed that eristostatin significantly impaired wound closure *in vitro* by C8161 human melanoma cells (McLane et al., 2005). We have confirmed this finding with four additional melanoma cell lines and identified αv as an integrin subunit involved in the interaction with some, but not all, melanoma cells lines used. Structurally, both the RGD motif and residues within both the N- and C-terminus of eristostatin are critical for this interaction.

2. Materials and methods

2.1. Materials

Human melanoma cell lines 1205 Lu (metastatic), WM164 (vertical growth phase) and SBcl2 (radial growth phase) cells were kindly provided by Dr. Meenhard Herlyn (Wistar Institute, Philadelphia, PA). Metastatic cell lines C8161 and MV3 were obtained from Fred Meyskens (University of California, Irvine Cancer Center) and Goos N.P.van Muijen (University Medical Center, Nijmegen, The Netherlands), respectively. M24met cells (metastatic) were from Ralph Reisfeld (The Scripps Institute, San Diego, CA). Dulbecco's modified eagle's medium/ham's F12 50:50 mix (DMEM) and Dulbecco's phosphate buffered saline (DPBS) were obtained from Mediatech (Herndon, VA), fetal bovine serum (FBS) was from GibcoBRL (Rockville, MD). Crude venom was obtained from Latoxan (Rosans, France). Albumin from bovine serum (BSA) was purchased from Sigma (St.Louis, MO). Fibronectin-coated 6-well plates were obtained from BD Biosciences (Bedford, MA), and 96-well PRO-BIND plates, from Becton Dickinson Labware (Franklin Lakes, NJ). Agar was purchased from BioRad Laboratories (Hercules, CA). Functional blocking antibodies against integrin αv (clone M9, Cat. #MAB1980) and β1 (clone P5D2, Cat. #MAB 1959) chains were purchased from Chemicon (Temecula, CA). Transwell filters, 8.0 µm pore size and 6.5 mm in diameter, were obtained from Costar (Cambridge, MA).

2.2. Cell culture

All cell lines were maintained in DMEM containing 10% FBS at 37 °C and 5% CO_2. Cells were grown to 80–90% confluence, detached using 2 mM EDTA, and centrifuged at $1200g$ for 5 min. After removal of media, cells were suspended in DPBS for use in proliferation and soft agar assays. For wound closure, time lapse, adhesion, and transwell migration assays, cells were washed twice and were resuspended with serum-free DMEM.

2.3. Preparation of native eristostatin and echistatin, recombinant eristostatin, and eristostatin mutants

Native eristostatin and echistatin were isolated from crude venom of *E. macmahoni* and *Echis carinatus sochurecki*, respectively, by high performance liquid chromatography (HPLC) on a C-18 reversed phase column developed with an acetonitrile gradient as previously described (McLane et al., 1994).

Wild-type and mutant recombinant eristostatin were expressed in *E. coli* by a modification of the method previously described (Wierzbicka-Patynowski

et al., 1999). Modification included the use of pET 39b (+) expression plasmid and isolation of the 6-histidine fusion protein with the His*Bind columns (Novagen, Madison, WI). Recombinant eristostatin clones were sequence-verified (DNA Sequencing Facility, University of Delaware, DE). Purity of recombinant eristostatin was assessed by SDS-PAGE, and molecular weight was confirmed by mass spectrometric analysis (Chemistry and Biochemistry Department, University of Delaware, DE).

2.4. Transwell migration assay

Transwell filters were equilibrated in serum-containing DMEM for 2 h before use. DMEM containing 10% FBS was added to the lower compartments of the migration filters. In a volume of 100 μl serum-free DMEM, 2×10^4 cells were plated per transwell filter. Cells were allowed to migrate for 6 h at 37 °C in 5% CO_2, and were subsequently fixed by immersion of the filters in methanol for 15 min at room temperature. Filters were washed once with water, and were stained in 0.2% crystal violet in a 20% methanol/water solution for 10 min. Cells were removed from the upper surface of the membrane with a cotton swab. Cells that had migrated to the underside of the membrane were counted at $200 \times$ magnification from five random fields per membrane.

2.5. In vitro wound closure assays

Cells (2×10^6/well) were plated on fibronectin-coated 6-well plates. After serum starvation for 24 h, the cells were scraped with a sterile 200 μl pipette tip and were washed twice with cold DPBS. Serum-free DMEM with or without eristostatin (0.5–3 μM) was added to each well. Measurements of the gap distance were taken with an ocular micrometer at each time point. The percent closure of untreated control was taken to be 100%. The percent closure of treated cells was calculated by dividing the distance that treated cells had migrated by the distance that untreated cells had migrated. A minimum of 9 observations for each cell type was made.

2.6. Time-lapse microscopy

Time-lapse wound closure assays were performed as described previously (Cretu et al., 2005). In brief,

cells were prepared and removed as described above using 3 μM eristostatin, and then abraded wells were placed in a custom culture chamber (37 °C and 5% CO_2) on a Nikon TE-2000E microscope. A Photometrics CoolSnap ES CCD camera (Roper Scientific, Inc.) was used to capture images on each plate at 5 min intervals for approximately 20 h under a $20 \times$ objective lens. Motility of cells was measured after collection of sequential time-lapse images. Cells which migrated back into the monolayer were excluded from the data collection. Analyses were performed on sequential phase-contrast images with MetaMorph software (Molecular Devices Corporation) manually using the "Track Points" feature, with individual nucleoli serving as imaging targets. Tabulated data were exported into Microsoft Excel, graphed, and evaluated statistically according to Student's two-tailed *t*-test.

2.7. Cell adhesion

PRO-BIND plates were coated with either recombinant eristostatin (1 μg in 100 μl) or 1% BSA and were incubated overnight at 4 °C. Plates were then blocked with 3% BSA in DMEM overnight at 4 °C, and were washed twice with DMEM containing 0.1% BSA. Cells were washed as described above and resuspended in DMEM containing 0.1% BSA at 2×10^5 cells/ml. The cells were preincubated for 15 min at room temperature with function-blocking mAbs against human integrin αv or β1 (10 μg/ml). Cells were added to the coated wells (2×10^4 cells per well) and allowed to attach for 1 h at 37 °C, 5% CO_2. Wells were washed twice with warm DMEM containing 0.1% BSA, and the attached cells were stained with 0.2% crystal violet in 20% methanol for 10 min. After washing, 0.5% Triton X-100 was used to lyse the cells and the absorbance was measured at 560 nm. Nonspecific binding (BSA-only wells) was subtracted from all values.

2.8. Proliferation assays

Cells (5×10^3) were plated in 96-well plates in 10% serum-containing medium with or without 3 μM eristostatin for 0, 24 or 48 h. Cell proliferation was determined by the 3-(4,5-dimethylthiazol-2-yl)-5-(3-carboxymethoxyphenyl)-2-(4-sulfophenyl)-2H-tetrazolium (MTS) assay (Promega, Madison, WI) according to the manufacturer's instructions.

2.9. Soft agar assays

Underlayers of 0.6% agar medium (1 ml) were prepared in 6-well plates by combining equal volumes of 1.2% noble agar and $2 \times$ DMEM with 20% FBS. 5×10^3 cells were plated in 0.3% agar medium with or without $3 \mu M$ eristostatin. The surface was kept wet by addition of a small amount of DMEM containing 10% FBS. After 14 days, colonies formed were stained with 0.005% crystal violet and were counted at $25 \times$ magnification.

2.10. Angiogenesis in the embryonic quail chorioallantoic membrane (CAM)

Fertilized Japanese quail eggs (*Coturnix coturnix japonica*), cleaned with 70% ethanol, were maintained at $37 \,^{\circ}C$ until embryonic day 3. The shells were opened with a razor blade and sterile scissors, and the contents were transferred into 6-well tissue culture plates prior to their return to the $37 \,^{\circ}C$ incubator. At embryonic day 8, 0.5 ml of test compounds in PBS (20, 66 and $166 \mu g/ml$) was applied drop-wise to coat the surface of the CAM, which covers the embryo, and were incubated for another 24 h. As the quail is not an inbred strain, there was some variability among embryos in the rate of growth and response to the test compounds. CAMs from eyeless or under-sized embryos were not used. After 24 h (on embryonic day 9), embryos were fixed with 5 ml of prewarmed 2% gluteraldehyde, 4% paraformaldehyde in PBS for 48 h at room temperature. Fixed CAMs were dissected from the surface of the embryo and mounted on glass slides in 10% polyvinyl alcohol, 25% glycerol in 0.5 M Tris, pH 8.5. The dried, mounted CAMs were photographed with a Nikon Microphot-SA digital camera microscope at $10 \times$ magnification. One $0.5 \, cm^2$/slide was recorded as an Adobe Photoshop image. No staining was necessary, as the arteries retained enough blood to render them semi-opaque. For comparison of arterial branching, composite figures were made from images that had been edited to remove veins and background. One field from each of three membranes per test solution was examined (Parsons-Wingerter et al., 1998).

2.11. Platelet aggregation

Disintegrin activity was screened by performing platelet aggregation with an ADP ($20 \mu M$) agonist, and was quantified by calculation of the IC_{50}. Aspirin-free blood was collected from healthy donors in 3.2% (w/v) sodium citrate (1:9 ratio), and was centrifuged at $1300g$ for 10 min. Platelet-rich plasma was separated from the cells within 30 min of collection. The concentration of each recombinant or native disintegrin that inhibited platelet aggregation by 50% was determined as described previously (Williams et al., 1990).

3. Results

3.1. Migration of melanoma cells

To assess cell mobility in response to eristostatin, we performed transwell migration assays using serum-containing medium as the attractant in the lower well. As shown in Fig. 1, the number of cells which migrated after exposure to eristostatin was significantly less than the control group for all melanoma cell lines.

The *in vitro* wound closure assays revealed a delayed closure on fibronectin matrix by eristostatin-treated human melanoma cells (Fig. 2(A)). Cells that were treated with $3 \mu M$ eristostatin closed 56–88% of the area in comparison with untreated control cells on fibronectin matrix. Eristostatin had no effect on closure of MV3, 1205Lu, M24met or C8161 on laminin or collagen IV, with the exception
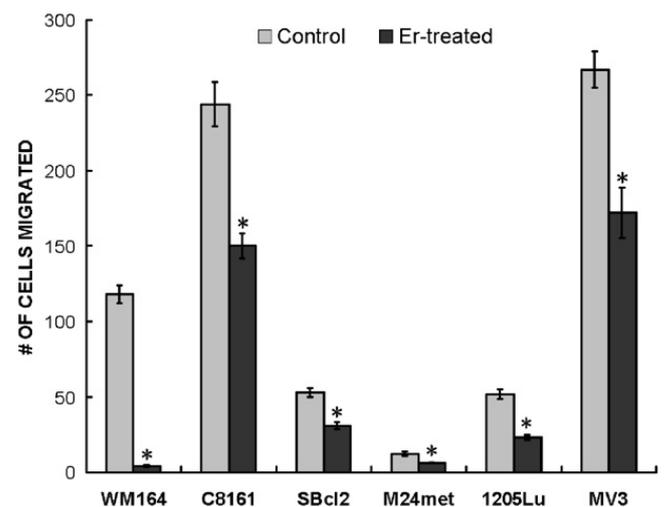

Fig. 1. Inhibition of cell migration by eristostatin. Indicated melanoma cells were plated on a transwell filter in the presence or absence of $3 \mu M$ eristostatin and allowed to migrate for 6 h. Migrated cells were counted microscopically. Data represents mean $\pm$ standard error from two experiments (five random fields per experiment), $*p < 0.05$, Er—eristostatin.
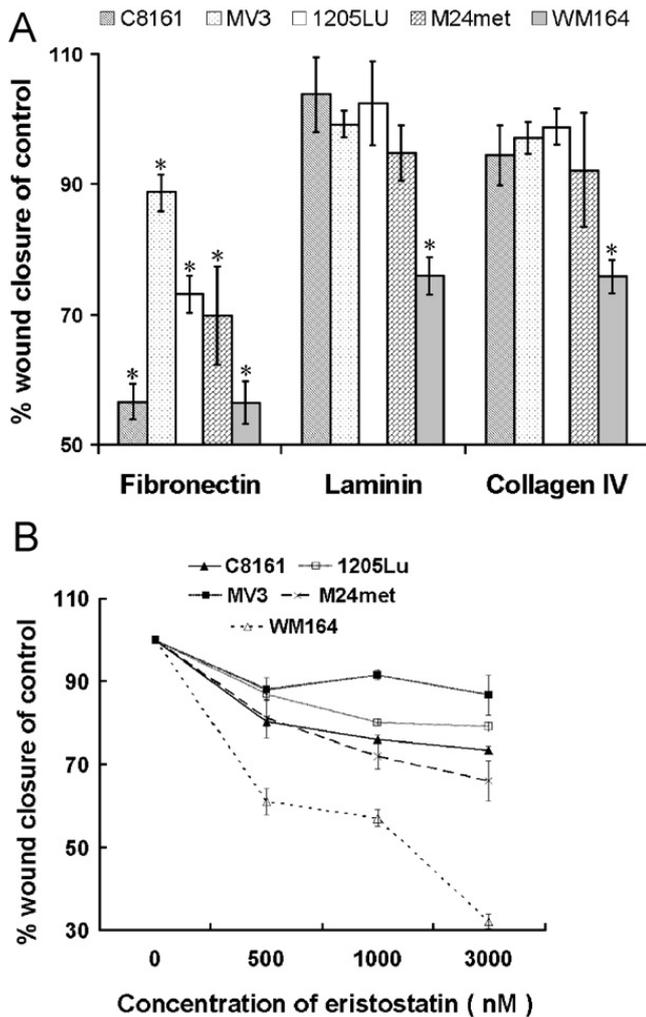
Fig. 2. (A) *In vitro* wound closure assays on different ECM. The closure of untreated control was taken to be 100%. The percent of control was calculated by dividing the distance that treated cell had migrated by the distance that untreated cells had migrated. The values represent the means ($\pm$SE, vertical bars) of nine independent experiments. (B) Eristostatin inhibits *in vitro* closure of melanoma cells on fibronectin matrix in a concentration-dependent manner. The percent wound closures of treated cells was calculated as above. The values represent the means ($\pm$SE, vertical bars) of nine independent experiments, *$p < 0.05$.

of WM164. In the presence of different concentrations of recombinant eristostatin, migration of cells on fibronectin was affected by eristostatin in a concentration-dependent manner (Fig. 2(B)) for all cell lines.

To evaluate the migration rate of treated vs. untreated cells, we performed a time lapse wound closure assay, in which photographs were taken at 5 min intervals while cells were migrating into the abraded area (Fig. 3, (A)—untreated, (B)—treated). In contrast to motility of untreated cells, eristostatin-

treated cells exhibited a decreased rate, except for 1205Lu, which showed no difference in velocity between control and eristostatin treatment (Figs. 3(C) and (D), Movies 1–10).

3.2. Adhesion of melanoma cells

To determine which integrin subunit(s) was (were) involved in the interaction between eristostatin and the melanoma cells, we used function-blocking antibodies against integrin subunits αv and $\beta 1$ in an adhesion assay. Both anti-αv and $\beta 1$ IgGs showed an inhibitory effect on the adhesion of WM164 and SBcl2 cell lines to immobilized eristostatin, whereas only anti-αv inhibited C8161 and 1205Lu cell adhesion (Fig. 4). Neither antibody affected the adhesion M24met and MV3 cells.

3.3. Proliferation of melanoma cells

To determine whether eristostatin affected cell cycle, we measured the proliferation of cells by the use of an MTS assay. Eristostatin-treated cells showed no difference in cell number compared with control cells over 48 h (Fig. 5(A)). We next determined the effects of eristostatin on the growth of melanoma cells in a three-dimensional soft agar environment. Melanoma cells were plated with or without 3 μM eristostatin within soft agar and were incubated for 2 weeks. Fig. 5(B) shows that the number of colonies formed by eristostatin-treated cells was similar to that of control cells. These results demonstrate that eristostatin has no effect on cell proliferation.

3.4. Angiogenesis

To evaluate the effect of eristostatin on angiogenesis, fertilized Japanese quail eggs (embryonic day 8) were treated with PBS containing echistatin or eristostatin (20–166 μg/ml). Twenty-four hours later, the blood vessels formed in the embryonic quail CAM were counted. There was no significant decrease in viability of the embryos, compared to PBS controls, in CAMs treated with the disintegrins, at doses up to 166 μg/ml. A significant decrease in arterial vessel density was seen in CAMs treated with echistatin at all concentrations tested, based on general morphological examination. CAMs treated with eristostatin were essentially equivalent to vehicle control (Figs. 6(A) and (B)).
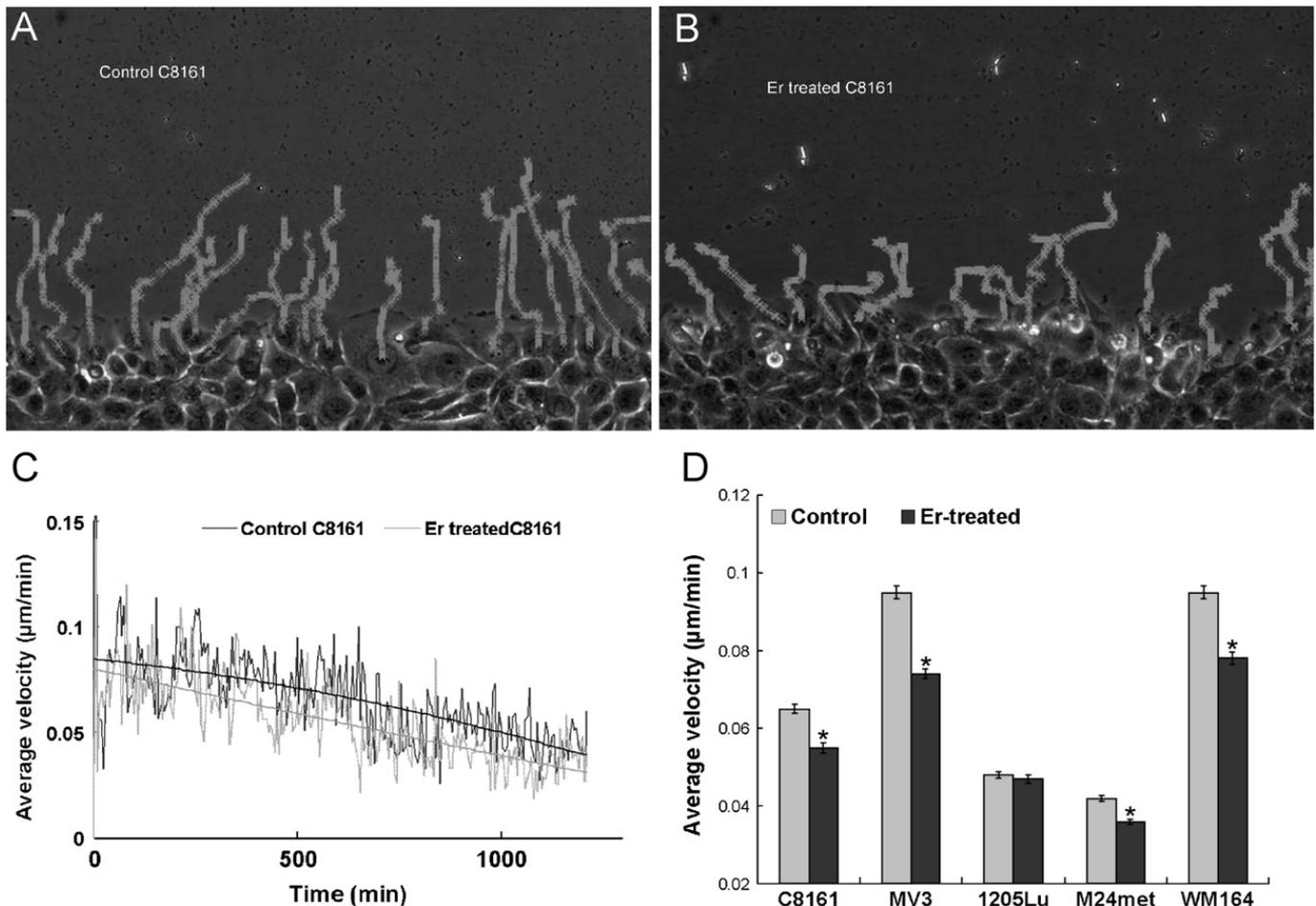
Fig. 3. Time-lapse microscopy. Cells were wounded on fibronectin-coated plates. (A) and (B): curved lines show the migration paths of C8161 cells at the leading edge; untreated (A) and treated with 3 μM eristostatin (B). (C) Same cells as in (A)/(B), plotted as average velocities over time with third-order curves of best fit. Dark upper line—control; gray lower line—eristostatin treated. (D) Average velocities of all cell lines. Data are averaged from about 40 cells/experiment. Bars indicate standard error; *$p < 0.05$ vs. control.
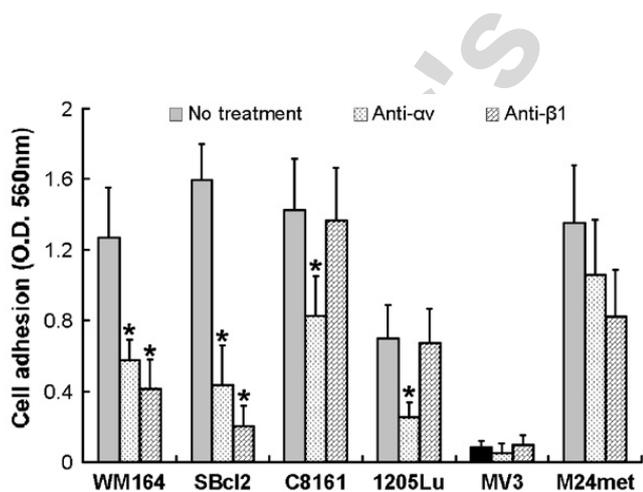

Fig. 4. Cell attachment on eristostatin (10 μg/ml) in response to functional blocking antibodies against integrin αv and β1. Each bar represents the mean ± SE of at least 8 wells, from 2 to 4 independent experiments. Nonspecific binding from BSA-coated wells was subtracted from all values, *$p < 0.05$ compared with no treatment.

3.5. Effect of alanine mutagenesis on eristostatin function

To identify residues critical for the function of eristostatin, we made mutations to alanine in the disintegrin, based on residues that differ from those in echistatin, a disintegrin that does not inhibit melanoma metastasis (Danen et al., 1998). The activities of the mutants were analyzed by in vitro wound closure assays and platelet aggregation. Residues Q1, E3 at the N-terminus, and D33 at the C-terminus, were not critical for the inhibition of cell migration of C8161 (Fig. 7(B)) or ADP-induced platelet aggregation (Fig. 7(A)), because they showed no significant differences from wild-type recombinant eristostatin in these two assays. In contrast, mutations of residues R24, V25, R27, G28, D29, W30 and N31 within the RGD loop, as well as
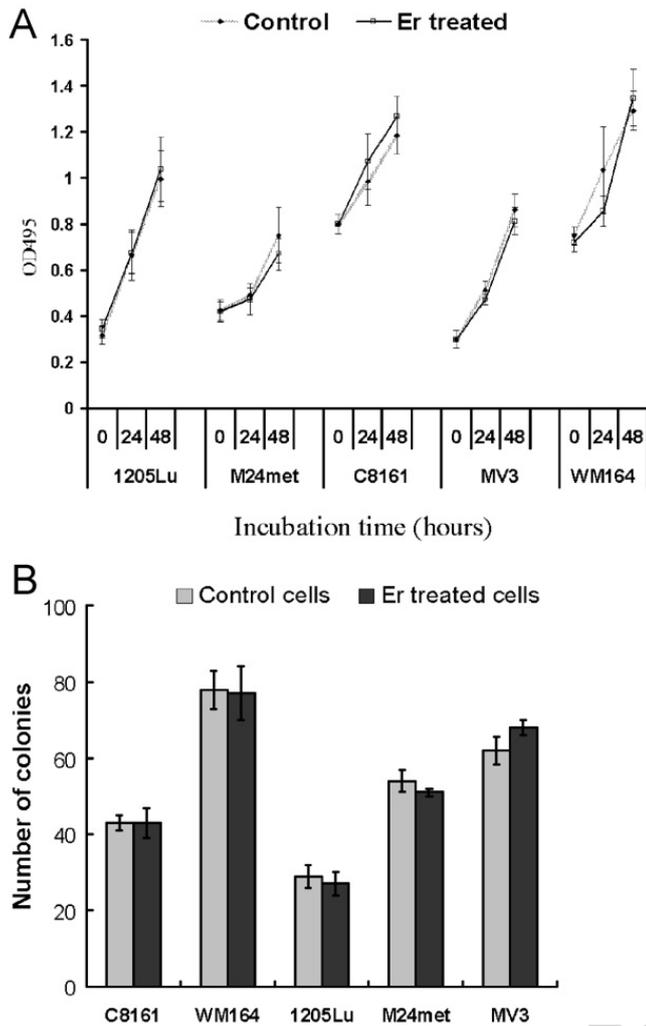
Fig. 5. Effect of eristostatin on cell proliferation. (A) MTS assay: cell proliferation is expressed as absorbance of formazan at 495 nm. Data represent the means $\pm$ S.E. for at least two experiments in duplicate. (B) Soft-agar assay: number of colonies are the mean $\pm$ SE of at least two experiments in which 5×10^3 cells were seeded per plate in triplicate.

K17, R18, S39 and D41, resulted in significantly blunted responses in both assays. Mutations of E2, T7, R13, W47, N48 and G49, which have IC_{50} values similar to those of wild type in ADP-induced platelet aggregation, lost their inhibition of wound closure *in vitro*. Mutations of P4, K21 and V22 affected only ADP-induced platelet aggregation.

4. Discussion

Many disintegrins, including echistatin (Hallak et al., 2005; Staiano et al., 1997), contortrostatin (Swenson et al., 2004; Trikha et al., 1994; Zhou et al., 2000), triflavin (Sheu et al., 1992, 1994), rhodostomin (Wiedle et al., 1999) and salmosin

(Kang et al., 2000) are effective anti-tumor agents *in vitro* and/or *in vivo*. The most common molecular mechanism has been an inhibition of angiogenesis through integrins $\alpha v\beta3$, $\alpha v\beta5$ or $\alpha5\beta1$. (Huang et al., 2001; Kang et al., 1999; Marcinkiewicz et al., 2003; Markland et al., 2001; Olfa et al., 2005; Yeh et al., 1998, 2001). Eristostatin has also been shown to inhibit lung or liver colonization *in vivo* by either human or murine melanoma cells (Beviglia et al., 1995; Danen et al., 1998; McLane et al., 2004; Morris et al., 1995). Our current data indicate that anti-angiogenesis cannot be a primary mechanism of eristostatin, because this disintegrin was not effective as an inhibitor of blood vessel growth in a CAM angiogenesis model (Fig. 6). Thus far, the only integrins linked functionally with eristostatin have been $\alpha IIb\beta3$ (McLane et al., 1994) and $\alpha4\beta1$ (Danen et al., 1998). It is unlikely, however, that either $\alpha IIb\beta3$ or $\alpha4\beta1$ are common targets since these receptors are not expressed on all melanoma cell types tested in these studies (Wong et al., 2002). The effect of eristostatin on cell migration was used in a screening assessment because this cellular activity is known to involve integrins. Inappropriate cell migration can also contribute to tumor cell metastasis. Eristostatin inhibited all melanoma cell lines tested in a transwell migration assay (Fig. 1). We previously reported that eristostatin significantly impaired *in vitro* wound closure of C8161 human melanoma cells plated on fibronectin (McLane et al., 2005). In this study, we have expanded that finding to include 4 additional human melanoma cell types: MV3, WM164, M24met, and 1205Lu, both at static time points (Fig. 2(A)) and through time-lapse experiments (Fig. 3, videos 1–10). This phenomenon was concentration dependent (Fig. 2(B)) and was selective for fibronectin in MV3, 1205Lu, M24met and C8161, all highly malignant melanoma cell lines (Fig. 2(A)). Only the less malignant, vertical growth phase WM164 melanoma cells were affected by eristostatin on fibronectin, laminin and collagen IV (Fig. 2(A)). Both cell migration and cell proliferation are important factors in this wound closure assay. Data from the MTS (Fig. 4(A)) and soft-agar assays (Fig. 4(B)) indicate that eristostatin has no effect on the proliferation of these melanoma cells, consistent with the study done by Morris et al. (1995) with B16F1 murine melanoma cells *in vitro*. These results strongly point to an effect of eristostatin only on cell migration, and a common mechanism involving fibronectin.
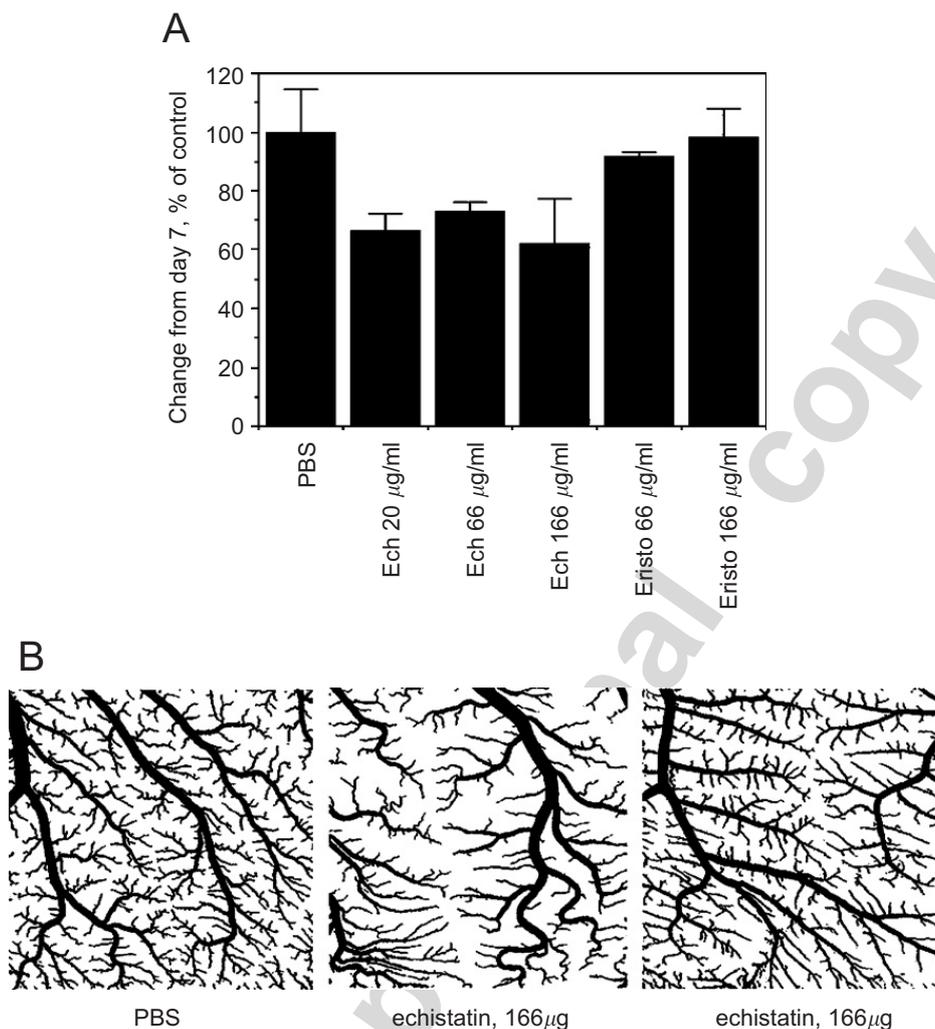
Fig. 6. Chorioallantoic membrane assay. (A) Change in arterial vessel fractal dimension on 8 day quail CAMs. Data are compiled from three membranes per condition. (B) Comparison of arterial vessel density. Ech—echistatin, Eristo—eristostatin.

Fibronectin is the major protein ligand of at least 12 integrins (Table 1) (Hynes, 2002; Plow et al., 2000), with nine recognizing the RGD sequence and three being nonRGD binding integrins. Previously we demonstrated that eristostatin abolishes the adhesion of melanoma cells to an immobilized RGD matrix (Pronectin-F®), a result favoring an RGD-dependent mechanism (McLane et al., 2005). In confirmation of this earlier observation, eristostatin lost its inhibitory effect on cell migration when residues R27, G28 and D29 were mutated (Fig. 7(B)). It is interesting, however, that the initial adhesion of MV3 and M24met cells to the Pronectin-F® plates was weaker than was observed with C8161, 1205Lu or WM164 cells; therefore, the activity of eristostatin on these cells plated on fibronectin might not depend solely on the RGD motif. Although mutations in the RGD loop of

eristostatin inhibit wound closure, it should be noted that alanine mutations of E2, T7 or R13 at the N-terminus, and W47, N48 or G49 at the C-terminus, also had a similar effect (Fig. 7(B)). A comparison of the lack of effect on platelet aggregation by these six amino acids (Fig. 7(A)) indicates that a different type of binding occurs with respect to the αIIbβ3 integrin involved in platelets and the integrin mediating melanoma cell migration. Of the nine RGD-dependent, fibronectin-binding integrins, it is unlikely that either αIIbβ3 or α5β1 is involved in interactions between eristostatin and the melanoma cells tested in this study. The fibrinogen receptor αIIbβ3 is not expressed on any of these cell lines (Wong et al., 2002). In addition, Beviglia et al. (1995), and our own laboratory (Pfaff et al., 1994; Wierzbicka-Patynowski et al., 1999), have shown that eristostatin
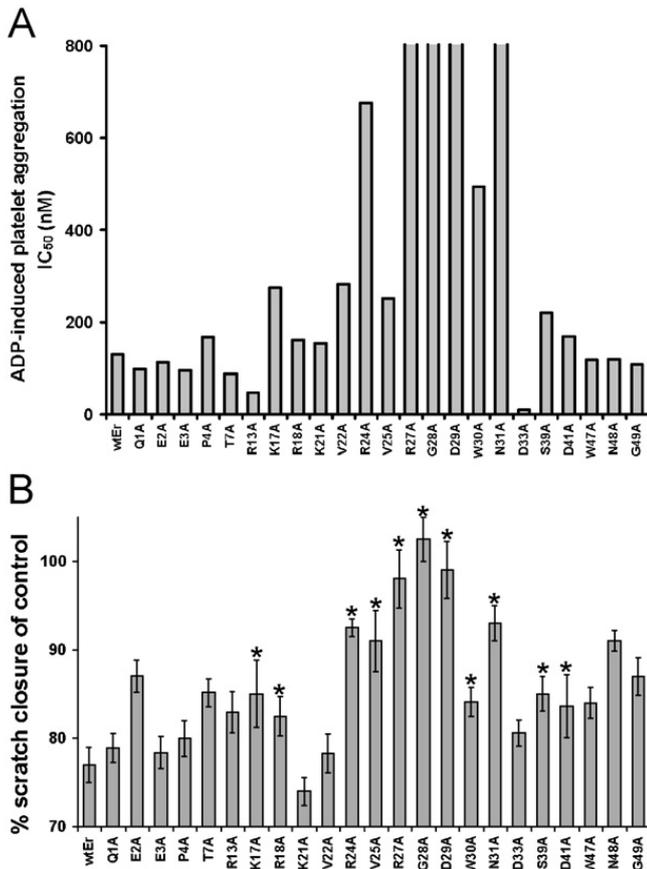
Fig. 7. Effect of eristostatin mutants in C8161 cell wound closure on fibronectin and on platelet aggregation. The same batch of recombinant eristostatin or its mutants was used to do both sets of experiments. (A) The IC_{50} values of R27, G28, D29 and N31 were infinity because those mutants showed no inhibitory effect on ADP-induced platelet aggregation. (B) Activities of mutants assayed by C8161 *in vitro* wound closure on fibronectin. The percent closure was calculated as previously described. The values represent the means ($\pm$SE, vertical bars) of nine independent experiments, wtEr—wild type eristostatin; each amino acid is represent by a single-letter code, * indicates mutations with significant loss of inhibition in both assays.

Table 1
Fibronectin-binding integrins

RGD dependent		nonRGD dependent
$\alpha3\beta1$	$\alpha v\beta3$	$\alpha2\beta1$
$\alpha5\beta1$	$\alpha IIb\beta3$	$\alpha4\beta1$
$\alpha8\beta1$	$\alpha v\beta5$	$\alpha4\beta7$
$\alpha v\beta1$	$\alpha v\beta6$	
	$\alpha v\beta8$	

interacts minimally, if at all, with $\alpha5\beta1$. Cell adhesion studies with antibodies to these integrin subunits (Fig. 4) indicate αv as a common target

for the interaction of C8161, WM164, SBcl2 and 1205Lu melanoma cells with eristostatin. It must be noted that the adhesion between eristostatin and MV3 or M24met is inhibited neither by anti-αv nor anti-$\beta1$ antibodies, so these cells must use different integrin binding partners. In addition, MV3 cells do not express the $\beta3$ subunit (Danen et al., 1998). Coupling this with the evidence that the latter two melanoma cell lines bound weakly to the RGD-based matrix on the Pronectin-F® plates suggests a potential nonRGD (and even nonintegrin) binding mechanism. These interesting possibilities are currently under investigation.

Acknowledgments

Appendix A. Supplementary Materials

Supplementary data associated with this article can be found in the online version at doi:10.1016/j.toxicon.2006.12.013.

References

Beviglia, L., Stewart, G.J., Niewiarowski, S., 1995. Effect of four disintegrins on the adhesive and metastatic properties of B16F10 melanoma cells in a murine model. Oncol. Res. 7, 7–20.

Couzin, J., 2003. Medicine: tracing the steps of metastasis, cancer's menacing ballet. Science 299, 1002–1006.

Cretu, A., Fotos, J.S., Little, B.W., Galileo, D., 2005. Human and rat glioma growth, invasion, and vascularization in a novel chick embryo brain tumor model. Clin. Exp. Metastasis 22, 225–236.

Danen, E.H., Marcinkiewicz, C., Cornelissen, I.M., van, K.A., Pachter, J.A., Ruiter, D.J., Niewiarowski, S., Van, M.G., 1998. The disintegrin eristostatin interferes with integrin alpha 4 beta 1 function and with experimental metastasis of human melanoma cells. Exp. Cell Res. 238, 188–196.

Giancotti, F.G., 1997. Integrin signaling: specificity and control of cell survival and cell cycle progression. Curr. Opin. Cell Biol. 9, 691–700.

Gould, R.J., Polokoff, M.A., Friedman, P.A., Huang, T.F., Holt, J.C., Cook, J.J., Niewiarowski, S., 1990. Disintegrins: a family of integrin inhibitory proteins from viper venoms. Proc. Soc. Exp. Biol. Med. 195, 168–171.

Hallak, L.K., Merchan, J.R., Storgard, C.M., Loftus, J.C., Russell, S.J., 2005. Targeted measles virus vector displaying echistatin infects endothelial cells via alpha(v)beta3 and leads to tumor regression. Cancer Res. 65, 5292–5300.

Huang, T.F., Yeh, C.H., Wu, W.B., 2001. Viper venom components affecting angiogenesis. Haemostasis 31, 192–206.

Hynes, R.O., 2002. Integrins: bidirectional, allosteric signaling machines. Cell 110, 673–687.

Jin, H., Varner, J.A., 2004. Integrins: roles in cancer development and as treatment targets. Br. J. Cancer 90, 561–565.

Kang, I.C., Lee, Y.D., Kim, D.S., 1999. A novel disintegrin salmosin inhibits tumor angiogenesis. Cancer Res. 59, 3754–3760.

Kang, I.C., Kim, D.S., Jang, Y., Chung, K.H., 2000. Suppressive mechanism of salmosin, a novel disintegrin in B16 melanoma cell metastasis. Biochem. Biophys. Res. Commun. 275, 169–173.

Marcinkiewicz, C., Weinreb, P.H., Calvete, J.J., Kisiel, D.G., Mousa, S.A., Tuszynski, G.P., Lobb, R.R., 2003. Obtustatin: a potent selective inhibitor of alpha1beta1 integrin in vitro and angiogenesis in vivo. Cancer Res. 63, 2020–2023.

Markland, F.S., Shieh, K., Zhou, Q., Golubkov, V., Sherwin, R.P., Richters, V., Sposto, R., 2001. A novel snake venom disintegrin that inhibits human ovarian cancer dissemination and angiogenesis in an orthotopic nude mouse model. Haemostasis 31, 183–191.

McLane, M.A., Kowalska, M.A., Silver, L., Shattil, S.J., Niewiarowski, S., 1994. Interaction of disintegrins with the alpha IIb beta 3 receptor on resting and activated human platelets. Biochem. J. 301, 429–436.

McLane, M.A., Paquette-Straub, C., Wong, A., Srivastava, A., Miele, M.E., 2003. Effect of the disintegrin eristostatin on hematogenous metastasis in three models of human malignant melnaoma. Proc. Am. Assoc. Cancer Res. 44, 1180 (abstract #5911).

McLane, M.A., Sanchez, E.E., Wong, A., Paquette-Straub, C., Perez, J.C., 2004. Disintegrins. Curr Drug Targets Cardiovasc. Haematol. Disord. 4, 327–355.

McLane, M.A., Zhang, X., Tian, J., Zelinskas, C., Srivastava, A., Hensley, B., Paquette-Straub, C., 2005. Scratching below the surface: wound healing and alanine mutagenesis provide unique insights into interactions between eristostatin, platelets and melanoma cells. Pathophysiol. Haemost. Thromb. 34, 164–168.

Morris, V.L., Schmidt, E.E., Koop, S., MacDonald, I.C., Grattan, M., Khokha, R., McLane, M.A., Niewiarowski, S., Chambers, A.F., Groom, A.C., 1995. Effects of the disintegrin eristostatin on individual steps of hematogenous metastasis. Exp. Cell Res. 219, 571–578.

Olfa, K.Z., Jose, L., Salma, D., Amine, B., Najet, S.A., Nicolas, A., Maxime, L., Raoudha, Z., Kamel, M., Jacques, M., Jean-Marc, S., Mohamed el, A., Naziha, M., 2005. Lebestatin, a disintegrin from Macrovipera venom, inhibits integrin-mediated cell adhesion, migration and angiogenesis. Lab. Invest. 85, 1507–1516.

Ouyang, C., Yeh, H.I., Huang, T.F., 1983. A potent platelet aggregation inhibitor purified from Agkistrodon halys (mamushi) snake venom. Toxicon 21, 797–804.

Parsons-Wingerter, P., Lwai, B., Yang, M.C., Elliott, K.E., Milaninia, A., Redlitz, A., Clark, J.I., Sage, E.H., 1998. A novel assay of angiogenesis in the quail chorioallantoic membrane: stimulation by bFGF and inhibition by angiostatin according to fractal dimension and grid intersection. Microvasc. Res. 55, 201–214.

Pfaff, M., McLane, M.A., Beviglia, L., Niewiarowski, S., Timpl, R., 1994. Comparison of disintegrins with limited variation in the RGD loop in their binding to purified integrins alpha IIb beta 3, alpha V beta 3 and alpha 5 beta 1 and in cell adhesion inhibition. Cell Adhes. Commun. 2, 491–501.

Plow, E.F., Haas, T.A., Zhang, L., Loftus, J., Smith, J.W., 2000. Ligand binding to integrins. J. Biol. Chem. 275, 21785–21788.

Ridley, A.J., Schwartz, M.A., Burridge, K., Firtel, R.A., Ginsberg, M.H., Borisy, G., Parsons, J.T., Horwitz, A.R., 2003. Cell migration: integrating signals from front to back. Science 302, 1704–1709.

Sheu, J.R., Lin, C.H., Chung, J.L., Teng, C.M., Huang, T.F., 1992. Triflavin, an Arg–Gly–Asp-containing antiplatelet peptide inhibits cell–substratum adhesion and melanoma cell-induced lung colonization. Jpn. J. Cancer Res. 83, 885–893.

Sheu, J.R., Lin, C.H., Huang, T.F., 1994. Triflavin, an antiplatelet peptide, inhibits tumor cell–extracellular matrix adhesion through an arginine–glycine–aspartic acid-dependent mechanism. J. Lab. Clin. Med. 123, 256–263.

Staiano, N., Garbi, C., Squillacioti, C., Esposito, S., Di Martino, E., Belisario, M.A., Nitsch, L., Di Natale, P., 1997. Echistatin induces decrease of pp125FAK phosphorylation, disassembly of actin cytoskeleton and focal adhesions, and detachment of fibronectin-adherent melanoma cells. Eur. J. Cell Biol. 73, 298–305.

Swenson, S., Costa, F., Minea, R., Sherwin, R.P., Ernst, W., Fujii, G., Yang, D., Markland Jr., F.S., 2004. Intravenous liposomal delivery of the snake venom disintegrin contortrostatin limits breast cancer progression. Mol. Cancer Ther. 3, 499–511.

Trikha, M., De Clerck, Y.A., Markland, F.S., 1994. Contortrostatin, a snake venom disintegrin, inhibits beta 1 integrin-mediated human metastatic melanoma cell adhesion and blocks experimental metastasis. Cancer Res. 54, 4993–4998.

Wiedle, G., Johnson, L.C., Imhof, B.A., 1999. A chimeric cell adhesion molecule mediates homing of lymphocytes to vascularized tumors. Cancer Res. 59, 5255–5263.

Wierzbicka-Patynowski, I., Niewiarowski, S., Marcinkiewicz, C., Calvete, J.J., Marcinkiewicz, M.M., McLane, M.A., 1999. Structural requirements of echistatin for the recognition of alpha vbeta 3 and alpha 5beta 1 integrins. J. Biol. Chem. 274, 37809–37814.

Williams, J., Rucinski, B., Holt, J., Niewiarowski, S., 1990. Elegantin and albolabrin purified peptides from viper venoms: homologies with the RGDS domain of fibrinogen and von Willebrand factor. Biochim. Biophys. Acta 1039, 81–89.

Wong, A., Paquette-Straub, C., McLane, M.A., 2002. Potential receptors for the binding of eristostatin to melanoma cells. In: Experimental Biology Annual Meeting Poster Abstract 146.5.

Yeh, C.H., Peng, H.C., Huang, T.F., 1998. Accutin, a new disintegrin, inhibits angiogenesis in vitro and in vivo by acting as integrin alphavbeta3 antagonist and inducing apoptosis. Blood 92, 3268–3276.

Yeh, C.H., Peng, H.C., Yang, R.S., Huang, T.F., 2001. Rhodostomin, a snake venom disintegrin, inhibits angiogenesis elicited by basic fibroblast growth factor and suppresses tumor growth by a selective alpha vbeta 3 blockade of endothelial cells. Mol. Pharmacol. 59, 1333–1342.

Zhou, Q., Sherwin, R.P., Parrish, C., Richters, V., Groshen, S.G., Tsao-Wei, D., Markland, F.S., 2000. Contortrostatin, a dimeric disintegrin from Agkistrodon contortrix contortrix, inhibits breast cancer progression. Breast Cancer Res. Treat. 61, 249–260.